Multi-Jet Production and Multi-Scale QCD

Z. Czyczula[1,2], *G. Davatz*[3], *A. Nikitenko*[4], *E. Richter-Was*[1,5,*], *E. Rodrigues*[6], *N. Tuning*[6]

[1] Institute of Physics, Jagiellonian University, Krakow, Poland
[2] Niels Bohr Institute, University of Copenhagen, Copenhagen, Denmark
[3] Institute for Particle Physics, ETH Zürich, Switzerland
[4] Imperial College, London, UK
[5] Institute of Nuclear Physics PAN, Krakow, Poland
[6] NIKHEF, Amsterdam, The Netherlands

Abstract

We summarize the contributions in Working Group II on "Multi-jet final states and energy flows" related to the topic of jet production, multi-jet topologies and multi-scale QCD. Different parton shower models will lead to systematic differences in the event topology. This may have a significant impact on predictions for the LHC. Here we will look at a few examples, such as the acceptance of $H \to \tau\tau$ events and in applying a jet veto in the non-hadronic $H \to WW \to l\nu l\nu$ decay channel. We also study the effect of CCFM evolution on the jet veto and on the event topology at the LHC in the forward region. Finally, we show that the choice of the QCD scale leads to large uncertainties in e.g. the $H \to \tau\tau$ analysis.

1 Introduction

In simulating high-energy interactions, the sequence of branchings such as $q \to qg$, can be modelled by calculating the exact amplitude of the Feynman diagrams, known as the matrix-element method, or, alternatively, can be modelled using the parton-shower approach. Matrix elements are in principle the exact approach but lead to increasingly complicated calculations in higher orders, and are therefore only used for specific exclusive physics applications, such as background estimates with multiple hard jets (see also [1]).

Since no exact way of treating partonic cascades exist, various Monte Carlo programs model the parton showers in different ways. In HERWIG [2] the parton showers are performed in the soft or collinear approximation, treating the soft gluon emission correctly. The shower is strictly angular ordered, where the angle between emitted partons is smaller at each branching. The hardest gluon emission is then matched to the first order matrix-element. This matrix-element correction has recently been implemented for $gg \to H$, leading to harder jets, and thus a more stringent jet veto in e.g. the non-hadronic decay $H \to WW \to l\nu l\nu$, where the jet veto is crucial to reduce the top background. PYTHIA [3] applies the collinear algorithm with the cascade ordered according to the virtuality Q^2. Corrections to the leading-log picture using an angular veto, lead to an angular ordering of subsequent emissions. The initial parton branchings are weighted to agree with matrix-elements. ARIADNE [4] on the other hand, does not emit gluons from single partons, but rather from the colour dipoles between two dipoles, thus automatically including the coherence effects approximated by angular ordering in HERWIG. From the resulting two dipoles softer emission occurs, resulting in a p_T ordering of subsequent emissions. ARIADNE has proven to predict the event shapes at HERA accurately [5], and could be explored more widely for simulation studies for the LHC.

The way parton showers are implemented affects the emission of soft gluons, and therefore affect both the transverse momentum of the produced Higgs, as well as the p_T of the balancing jets. In the

following we will discuss the effect of the different parton showers on the selection of $H \to \tau\tau$ by applying angular cuts on the jets and on the selection of $H \to WW \to l\nu l\nu$ by rejecting events with jets with large p_T.

Both PYTHIA and HERWIG are general purpose leading order (LO) parton shower Monte Carlo programs, based on LO matrix elements. MC@NLO [6] on the other hand, uses exact next-to-leading order (NLO) calculations and is matched to the HERWIG parton shower Monte Carlo. Its total cross section is normalized to NLO predictions. The different predictions of these programs for the high part of the transverse momentum spectrum of the Higgs will be described in detail.

In the parton cascade as implemented in e.g. PYTHIA, the parton emissions are calculated using the DGLAP approach [7], with the partons ordered in virtuality. DGLAP accurately describes high-energy collisions of particles at moderate values of the Bjorken-x by resummation of the leading log terms of transverse momenta $((\alpha_s \ln Q^2)^n)$. However, to fixed order, the QCD scale used in the ladder is not uniquely defined. Different choices of the scale lead to large differences in the average transverse momentum of the Higgs in e.g. the processes $gb \to bH$ and $gg \to bbH$.

In the CCFM formalism [8] there is no strict ordering along the parton ladder in transverse energy, contrary to the DGLAP formalism. The CASCADE Monte Carlo program [9] has implemented the CCFM formalism, inspired by the low-x F_2 data and forward jet data from HERA, and became recently available for pp scattering processes. Until now, CASCADE only includes gluon chains in the initial state cascade. Different sets of unintegrated gluon densities are available, which all describe HERA data equally well [9]. Note, however, that it is questionable if these densities are constrained enough for Higgs production, as discussed elsewhere in these proceedings [10].

CCFM is expected to provide a better description of the gluon evolution at very low values of x compared to DGLAP, as it also takes leading-logs of longitudinal momenta $((\alpha_s \ln x)^n)$ into account. Since the partons at the bottom of the ladder (furthest away from the hard scatter) are closest in rapidity to the outgoing proton, effects might be expected in the forward region. The event topology in terms of jets and charged multiplicity is investigated at rapidities $2<\eta<5$, corresponding to the acceptance of the LHCb detector.

2 MSSM Higgs production with the Yukawa bbH coupling induced mechanisms

In the MSSM, the Yukawa coupling of the heavy neutral Higgs bosons to the bottom quarks is strongly enhanced for large tan(β) with respect its SM value, which makes the Higgs boson production in association with bottom quarks the primary production mechanism in LHC pp collisions. Currently, the inclusive cross section for this process is under good control up to NNLO, both in the so called fixed-flavour-scheme (FFS) and varying-flavour-scheme (VFS). The impressive level of theoretical uncertainty in the order of 15% is achieved on the predictions for the total cross-section for m_H=120 GeV [11, 12].

The observability potential for the $H \to \tau\tau$ channel [13] is, however, very sensitive to the topology of the events, due to the reconstruction of the invariant mass of the tau-pair, using the collinear approximation of τ-leptons decay, in order to account for the neutrino momenta. The impact of the event topology on the final acceptance of the signal has been discussed elsewhere [14]. Here, we pursue the subject further and we study more quantitatively the systematic effects from the parton shower model and the choice of the QCD scale selected in the event generation.

Currently available Monte Carlo generators for the Higgs boson production are based on the LO matrix elements, with the QCD part of physics event simulated with a parton shower approach. Clearly, the kinematics of the Higgs boson (and therefore the final acceptance for the signal) depends strongly on the algorithm used to simulate the QCD cascade. At tree level, the following exclusive processes have been studied, combining the observability of events with and without spectator b-tagged jets accompanying the reconstructed tau-pair: $gb \to bH$ (VFS), $gg \to b\bar{b}H$ (FFS), $b\bar{b} \to H$ (VFS) and $gg \to H$.

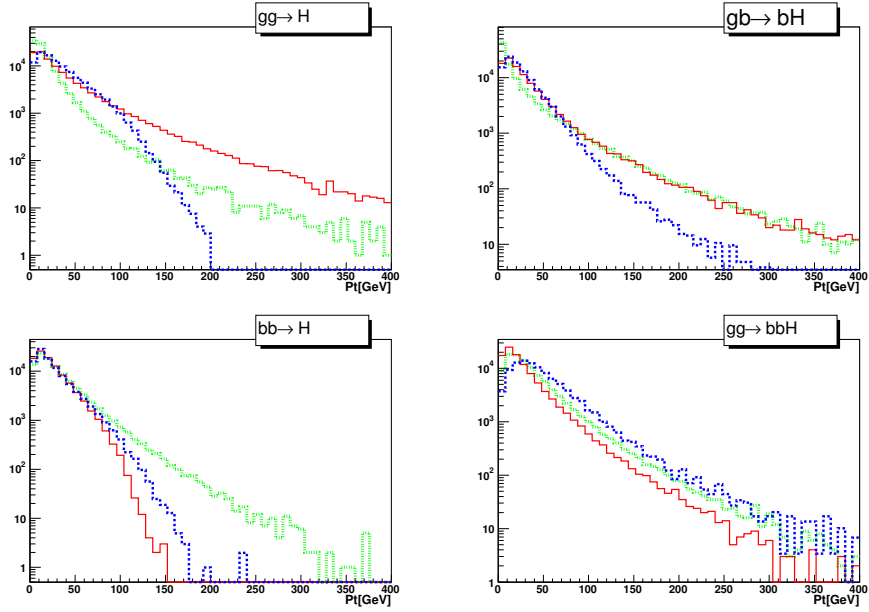For the purpose of the discussion presented here we have studied the SM Higgs boson production

Fig. 1: The transverse momenta of the Higgs boson, p_T^{Higgs} for 3 different shower models for each production mechanism. The red solid line represents PYTHIA, the dashed green line ARIADNE and the dotted blue line HERWIG events. The vertical scale gives the number of events per bin, and a total of 10^5 events have been generated with each program.

with a mass of 120 GeV, decaying into a tau pair, where one tau decays hadronically and one leptonically. The reconstruction of the Higgs boson mass and the selection criteria were performed at the level of generated particles (leptons, hadrons) or, where necessary (missing energy, b-jets), on objects reconstructed from simplified simulation of the detector response [15].

2.1 Systematics from the choice of parton shower model

As discussed in the introduction, the various parton shower models predict different spectra of the transverse momentum, p_T^{Higgs}, of the produced Higgs boson. This leads to a large variation in the prediction for the fraction of accepted events. The obvious starting point for the discussion is the Higgs boson transverse momentum spectra in complete physics events [1]. In case of the 2→2 and 2→3 processes, the p_T of the Higgs boson arrises predominantly from matrix elements, whereas in the 2→1 events p_T^{Higgs} purely comes from the parton shower. Therefore, the Higgs transverse momentum spectra differ significantly for different models of the QCD cascade. Figure 1 shows these spectra for each production mechanism [2].

Clearly, the spectra of the Higgs boson transverse momenta show substantial dependence not only on the topology of the hard process, but also on the shower model used in the simulation of the event. The shower model as implemented in PYTHIA includes hard matrix element corrections for inclusive gluon-gluon fusion, $gg \rightarrow H$, hence leading to a harder spectrum compared to the one obtained from the standard HERWIG shower. In this production mode the shower model from ARIADNE fails because of the missing splitting kernel for $g \rightarrow q\bar{q}$. On the other hand, the ARIADNE model predicts the hardest spectra for the process $b\bar{b} \rightarrow H$. In this production channel, predictions from PYTHIA and HERWIG

---

[1]The AcerMC 2.4 framework [16] with interfaces to PYTHIA 6.2, ARIADNE 4.12 and HERWIG 6.5 was used to generate events and AcerDET [15] was used to simulate the detector performance.

[2]The CTEQ5L parton density functions were used in all simulations. It has been checked that both final acceptance of the signal and the mean Higgs boson transverse momentum is almost independent of the pdf parametrization. Uncertainties below 10% are observed by using CTEQ5L, CTEQ6L, MRST2001 interfaced with LHAPDF [17]).

Table 1: The average transverse momenta of the Higgs boson and acceptance of selection criteria for different hard processes and parton shower models. Events were generated with default initialization of these generators. Columns marked `PY`, `AR` and `HW` denote results from PYTHIA, ARIADNE and HERWIG shower model respectively.

Hard process	**gg → H**			**bb̄ → H**		
Shower model	PY	AR	HW	PY	AR	HW
$< p_T^{\text{Higgs}}$ (generated)$>$ (GeV)	37.2	X	32.2	23.1	29.9	24.6
$< p_T^{\text{Higgs}}$ (accepted)$>$ (GeV)	129.4	X	75.27	58.6	91.64	68.4
basic selection	14.2%	X	12.7%	12.8%	13.8%	11.8%
+($cos(\phi) >$-0.9 , $|sin(\phi)| >$0.2)	5.5%	X	4.5%	2.9%	4.3%	2.7%
+($p_T^{miss} > 30$ GeV, $m_T^{lep-miss} <$50GeV)	3.8%	X	2.3%	1.4%	2.3%	1.5%
+(mass window: 120 ± 20 GeV)	2.4%	X	1.3%	0.6%	1.3%	0.6%
+(1 tagged b-jet)				0.4%	1.0%	0.4%
Hard process	**gb → bH**			**gg → bb̄H**		
Shower model	PY	AR	HW	PY	AR	HW
$< p_T^{\text{Higgs}}$ (generated)$>$ [GeV]	32.5	26.0	26.9	27.2	35.8	47.4
$< p_T^{\text{Higgs}}$ (accepted)$>$ [GeV]	125.1	133.9	82.1	95.0	99.6	105.3
basic selection	13.3%	12.6%	11.7%	13.0%	13.6%	12.1%
+($cos(\phi) > -0.9, |sin(\phi)| >$0.2)	4.4%	3.4%	3.2%	3.5%	5.1%	6.7%
+($p_T^{miss} > 30$ GeV,$m_T^{lep-miss} <$50GeV)	2.7%	2.4%	1.7%	2.0%	2.9%	3.8%
+(mass window: 120 ± 20 GeV)	1.7%	1.5%	0.9%	1.1%	1.8%	2.6%
+(1 tagged b-jet)	1.3%	1.4%	0.6%	0.9%	1.2%	2.1%

are in quite good agreement. However, almost a factor of two difference for the prediction of the mean transverse momenta can be reported between PYTHIA and HERWIG in $gg \to b\bar{b}H$ process.

Numerical values for the average Higgs boson transverse momentum in different production processes and parton shower models are given in Table 1. It is important to stress that these results were obtained with default settings of the parameters for each parton shower model.

The steps of the analysis that lead to the reconstruction of the tau-pair invariant mass are indicated in Table 1, including the acceptances for all the discussed production processes and parton shower models. They consist of the basic selection (including the trigger and p_T and $|\eta|$ cuts on the lepton and jet), and the additional selection that is needed to improve the mass resolution of the accepted tau-pair. The acceptance of the signal after the basic selection is rather stable, at the level of 12%-14% depending on the production mechanism. The significant differences start to appear when a cut on the angle between the lepton and hadron is applied. A difference of almost a factor two is observed for the $b\bar{b} \to H$ production process with the parton shower from the HERWIG or ARIADNE model, respectively.

For the final acceptance values, the uncertainty from the parton shower model varies between 85% for inclusive gluon fusion to 135% for $gg \to bbH$ (between HERWIG and PYTHIA models). In the case of the Higgs production through $bb \to H$, predictions from HERWIG and PYTHIA models are in excellent agreement. However, the prediction of the acceptance in this production channel differs by 115% if the parton shower from ARIADNE is used. For the $gb \to bH$ production mechanism, the uncertainty due to the shower model from either PYTHIA or HERWIG is about 90%.
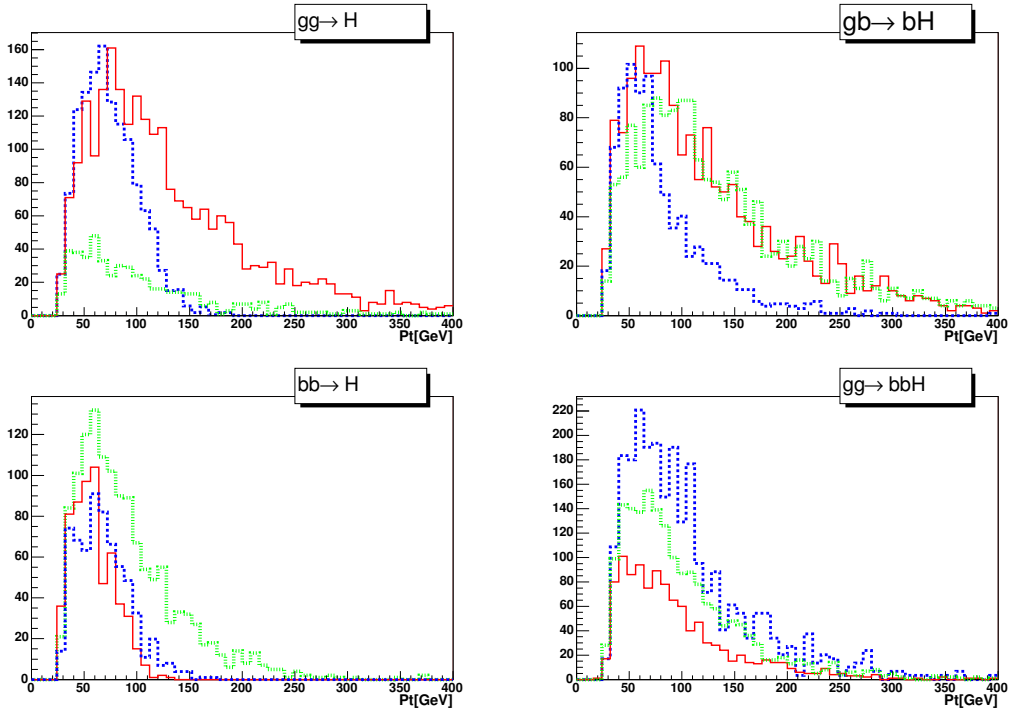
Fig. 2: Same as Fig. 1 but after selection presented in Table 1. The vertical scale in in number of events entering given bin after selection procedure, in each case 10^5 events were initially generated.

The systematic theoretical uncertainty on the predictions for the final acceptance ranges from 85% to 135% for the three different shower models studied here. The uncertainty is even larger, when the requirement of an additional tagging b-jet is introduced, up to 170% for $bb \rightarrow H$ [3]. Figure 2 shows the Higgs boson transverse momentum for those events that passed all selection criteria. As can be observed, the selection criteria rejected most of events with $p_T^{\text{Higgs}} < 40$ GeV.

2.2 Systematics from the choice of QCD scale

Having considered here the available Monte Carlo generators with the overall precision of the leading order only, large uncertainties are expected for the predictions coming from different scale choices. Here we concentrate only on the effects on the event topology, neglecting the effects from the choice of the QCD scale on the total cross-section. Table 2 shows the Higgs boson mean transverse momentum and final acceptance of the signal for 2→2 and 2→3 processes for some possible choices in PYTHIA and ARIADNE. The Q^2 value sets the scale not only for the hard scattering process, but also for the initial state parton shower. For the 2→1 production, the Q^2 scale is naturally set to be the mass of the Higgs boson mass. The uncertainty in the acceptance due to scale choice for the $gg \rightarrow b\bar{b}H$ production mechanism is about 60% in the case of PYTHIA and 25% in the case of ARIADNE parton shower model. For the exclusive process $gb \rightarrow bH$, the uncertainties are 75% and 100%, respectively.

3 gg → H at the LHC: Uncertainty due to a Jet Veto

In the Higgs mass range between 155 and 180 GeV, $H \rightarrow W^+W^- \rightarrow \ell\nu\ell\nu$ is considered to be the main Higgs discovery channel [18, 19]. The signal consists of two isolated leptons with large missing E_T and

---

[3]It should be stressed, that the problem of the efficiency of b-jet tagging was not touched upon, nor was the problem of the efficiency for the reconstruction of the τ-jet. Discussing these effects, very important for complete experimental analysis, would complicate the problem and dilute the aim of the phenomenological studies presented here.

Table 2: The average transverse momenta of the Higgs boson and acceptance of selection criteria for different scale choices. Events were generated with default initialization of these generators. Events marked `PY` and `AR` denote results from PYTHIA and ARIADNE shower model respectively.

Hard process	$\mathbf{gb \rightarrow bH}$			$\mathbf{gg \rightarrow b\bar{b}H}$			
Q^2 scale	default	$\hat{s}$	$\frac{2\hat{s}\hat{t}\hat{u}}{\hat{s}^2+\hat{t}^2+\hat{u}^2}$	default	m_b^2	m_b^2	$\hat{s}$
<Q> (GeV)	94	257	49	27	4.8	120	255
$< p_T^{\text{Higgs}}$ (generated)> (GeV)[PY]	32.5	42.7	43.2	27.2	29.8	32.1	36.2
Acceptance (%) [PY]	1.7	2.6	2.96	1.1	1.3	1.4	1.8
$< p_T^{\text{Higgs}}$ (generated)> (GeV)[AR]	26.0	25.5	44.9	35.8	38.	35.3	34.5
Acceptance (%) [AR]	1.5	1.6	3.1	1.8	2.1	1.7	1.7

with a small opening angle in the plane transverse to the beam, due to spin correlations of the W-pair. In order to reduce the top background, a jet veto has to be applied. The signal over background ratio is found to be around 2:1 for Higgs masses around 165 GeV. For lower and higher Higgs masses, the signal over background ratio decreases slightly [19]. The experimental cross section σ_{meas} of the Higgs signal and other final states is given by:

$$\sigma_{meas} = N_s/(\epsilon_{sel} \times L_{pp}), \tag{1}$$

with N_s being the number of signal events, ϵ_{sel} the efficiency after all signal selection cuts are applied and L_{pp} the proton-proton luminosity. In order to get an estimate of the cross section uncertainty, the statistical and systematic uncertainties have to be determined. The systematic uncertainties come from the experimental selection, background and luminosity uncertainties. As the signal over background ratio is small in the channel under study, the systematic uncertainties should be known precisely. This study concentrates on the uncertainty of the signal efficiency due to the jet veto, by studying the systematics using different Monte Carlo simulations. To do so, four different parton-shower Monte Carlo programs were used, as described in the introduction. The effect of different parton shower models are discussed by comparing PYTHIA 6.225 [3] and HERWIG 6.505 [2], whereas the comparison to MC@NLO 2.31 [6] leads to an uncertainty estimate of higher-order effects [4]. Then, also CASCADE 1.2009 [9] is studied to compare the DGLAP approach to the CCFM formalism.

Jets are reconstructed using an iterative cone algorithm with a cone size of 0.5. The leading particle (seed) of the jet is required to have a p_T larger than 1 GeV. The pseudo-rapidity $|\eta|$ of the jet should be smaller than 4.5, corresponding to the CMS detector acceptance [20]. The event is rejected if it contains a jet with a p_T higher than 30 GeV. The Higgs mass for this study was chosen to be 165 GeV, corresponding to the region of phase space with the highest signal over background ratio. First, all events are studied without considering the underlying event. Finally, PYTHIA is also studied including different underlying event schemes.

3.1 Matrix Element Corrections

At leading order, the transverse momentum of the Higgs boson, p_T^{Higgs}, is zero. However, parton shower Monte Carlos emit soft gluons which balance the Higgs and introduce a transverse momentum in LO parton shower Monte Carlos. As the Higgs is balanced by jets, the transverse momentum is very sensitive to the jet veto and therefore also the efficiency of a jet veto dependends stongly on p_T^{Higgs}.

In Fig. 3, the normalized p_T^{Higgs} spectra are shown for PYTHIA, HERWIG and MC@NLO. HER-WIG and MC@NLO are very similar at low p_T, as can be seen on the linear scale, which is to be expected as the soft and collinear emissions of MC@NLO are treated by HERWIG. Figure 4 shows that PYTHIA

---

[4]In the following, HERWIG and PYTHIA use the pdf-set CTEQ5L, whereas MC@NLO uses CTEQ5M.
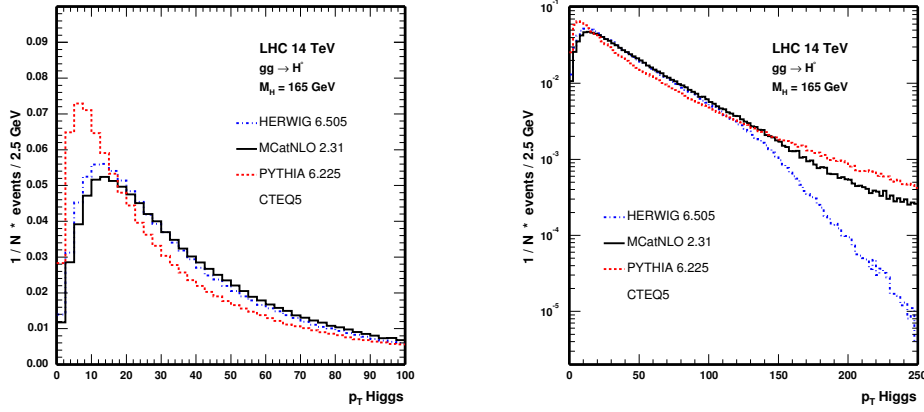
Fig. 3: p_T^{Higgs} spectra for PYTHIA, HERWIG and MC@NLO in linear and logarithmic scale.
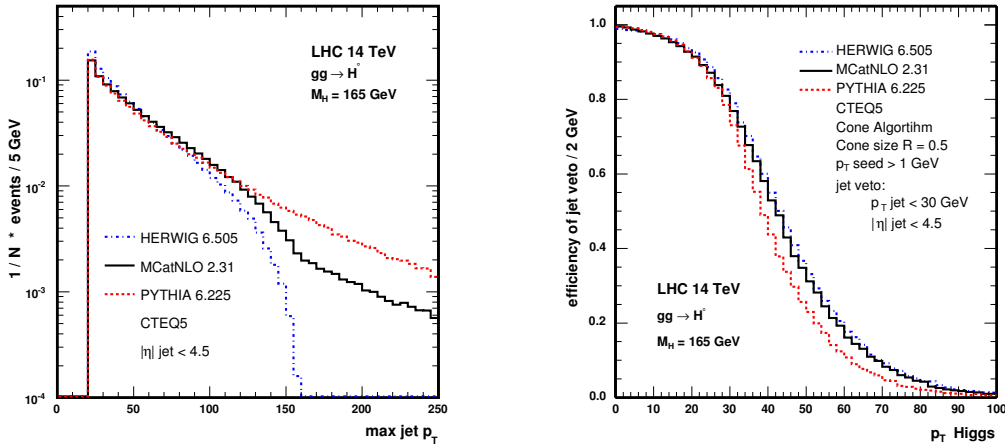

Fig. 4: p_T of the leading jet for PYTHIA, HER-WIG and MC@NLO

Fig. 5: Efficiency of the jet veto of 30 GeV as a function of p_T^{Higgs}.

predicts a softer leading jet spectrum than HERWIG and therefore also a softer p_T^{Higgs} spectrum. HERWIG implements angular ordering exactly and thus correctly sums the LL (Leading Log) and part of the $N^k LL$ (Next-to..Leading Log) contributions. However, the current version of HERWIG available does not treat hard radiations in a consistent way. Hence the spectrum drops quickly at high p_T, see Fig. 3b). PYTHIA on the other hand does not treat angular ordering in an exact way, but includes hard matrix element corrections. Therefore PYTHIA looks more similar to MC@NLO at high p_T. MC@NLO correctly treats the hard radiation up to NLO, combining the high p_T spectrum with the soft radiation of HERWIG.

In Fig. 5, the efficiency of the jet veto is shown for the three different Monte Carlos as a function of p_T^{Higgs}. One observes a strong dependency of p_T^{Higgs} on the jet veto. Once a jet veto is defined, the efficiency starts to drop quickly as soon as p_T^{Higgs} is close to the p_T used to define a jet veto. However, as the transverse momentum of the Higgs can be balanced by more than one jet, the efficiency is not zero above this value.

G. Corcella provided a preliminary version of HERWIG including hard matrix element corrections for $gg \rightarrow H$ [21]. The hard matrix element corrections lead to harder jets, see Fig. 6, and therefore the jet
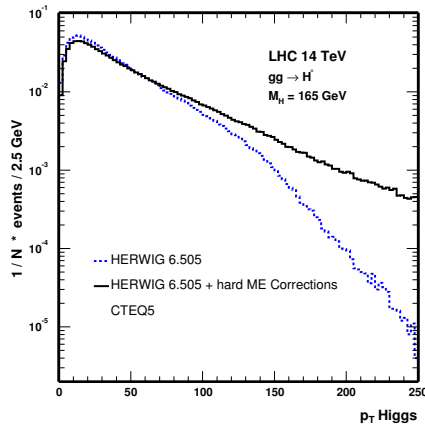
Fig. 6: HERWIG with and without hard Matrix Element Corrections, logarithmic scale.

Table 3: Efficiency of jet veto for MC@NLO, PYTHIA, HERWIG, HERWIG + ME Corrections and CASCADE

	Efficiency for events with a p_T Higgs between 0 and 80 GeV	Inclusive efficiency (all events)
MC@NLO 2.31	0.69	0.58
PYTHIA 6.225	0.73	0.62
HERWIG 6.505	0.70	0.63
HERWIG 6.505 + ME Corrections	0.68	0.54
CASCADE 1.2009	0.65	0.55

veto is more effective. At high p_T, PYTHIA and HERWIG now show very similar predictions. Table 3 shows the efficiencies of the jet veto of 30 GeV for MC@NLO, PYTHIA and HERWIG with and without matrix element corrections. In addition, the numbers for CASCADE are shown, which will be discussed in more detail later. In the first row, the number of the efficiency for p_T^{Higgs} between 0 and 80 GeV is shown. The second column shows the inclusive efficiency for all events. One has to keep in mind that after all selection cuts, only the low p_T region is important [19].

In order to estimate the effect from the detector resolution on the jet veto, the E_T of the jet is smeared with the jet resolution of e.g. CMS, as given by [20]:

$$\Delta E_T/E_T = 118\%/\sqrt{E_T} + 7\%. \tag{2}$$

More jets at initially low p_T are shifted to higher p_T than vice versa, as the jets are generally soft. However, the effect of the smearing is limited and the difference between the smeared and unsmeared case is smaller than 1%.

In the last years, a lot of progress has been made in understanding the Higgs boson production and decays on a theoretical basis. The gluon fusion cross section has been calculated up to NNLO [22]. Such corrections are known to increase the LO cross section by a factor of more than two. In order to include these higher order corrections in a parton shower Monte Carlo, each event is reweighted with its corresponding p_T-dependent effective K-factor (which includes all selection cuts) [19]. This technique can be applied to other processes which are sensitive to jet activity, e.g. the WW background for this channel. The result is an overall effective K-factor of 2.04 for a Higgs mass of 165 GeV, which is only

Table 4: Efficiency numbers for different underlying event tunings in PYTHIA.

	Efficiency for events with a p_T Higgs between 0 and 80 GeV	Inclusive efficiency (all events)
PYTHIA no UE	0.730	0.620
PYTHIA default	0.723	0.613
ATLAS tune	0.706	0.600
CDF tune	0.709	0.596

about 15% lower than the inclusive K-factor (without any cuts) for the same mass. This reweighting method allows to optimize the selection cuts and thus also helps to improve the discovery potential. We observe that the uncertaintiy of the jet veto efficiency does not change significantly including those higher order corrections.

3.2 Underlying Event

So far all events were generated without considering the underlying event. However, to study a jet veto, it is important to consider also the effect of the underlying event. Therefore, PYTHIA was studied with different underlying event tuning schemes, which are the ATLAS Tune [23], CDF Tune A [24] and PYTHIA default (MSTP(81)=1, MSTP(82)=3 [3]). The different tunings lead to approximately the same efficiency, and also the difference in the efficiency with and without underlying event is smaller than 1%, see Table 4.

3.3 Comparing to CCFM evolution

Finally, we compared the PYTHIA, HERWIG and MC@NLO predictions with the ones obtained using CASCADE. One has to keep in mind that this Monte Carlo is dedicated to low-x physics, and is about to be released for LHC physics applications. There were many improvements implemented during this workshop. In Fig. 7, the p_T^{Higgs} spectra for PYTHIA, HERWIG+ME Corrections, MC@NLO and CAS-CADE are shown. The prediction from CASCADE lies within the ones from PYTHIA and HERWIG. When looking at different p_T regions, one generally observes that CASCADE produces more jets compared to the other Monte Carlos, and the jets are harder. The jet veto efficiency as a function of the p_T of the Higgs is shown in Fig. 8, indicating that the main differences are in the low p_T range and that the efficiency for CASCADE is slightly smaller than unity at a p_T^{Higgs} of zero. A reason for this is that the Higgs boson is balanced by more than one jet, with at least one of the jets with a p_T higher than 30 GeV and thus vetoed. For the same reason, the efficiency in general is lower than for the other Monte Carlo programs at low p_T^{Higgs}. Results in the high p_T region have to be studied carefully.

4 Forward Studies with CASCADE at LHC Energies

The applicability of DGLAP evolution [7] is known to be limited in the very forward region, that is at small values of Bjorken-x, where $ln(x)$ terms are expected to become large [25]. Since the partons at the bottom of the ladder (furthest away from the hard scatter) are closest in rapidity to the outgoing proton, effects might be expected in the forward region. The CCFM evolution [8] takes these BFKL-like terms into account, and is implemented in the CASCADE Monte Carlo program [9].

We have studied the topology of forward particle and jet production in the LHCb detector at the LHC. LHCb is a forward spectrometer covering roughly the forward region $1.8<\eta<4.9$ [26]. Its main goal is the study of CP violation in the B-meson sector and the measurement of rare B-decays. But its very nature makes LHCb a suitable environment for QCD forward studies.
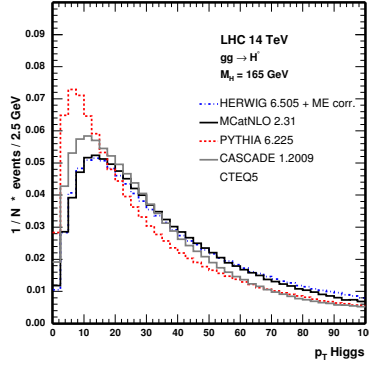
Fig. 7: p_T^{Higgs} Higgs of PYTHIA, HERWIG + ME Corrections, MC@NLO and CASCADE, linear and logarithmic scale.
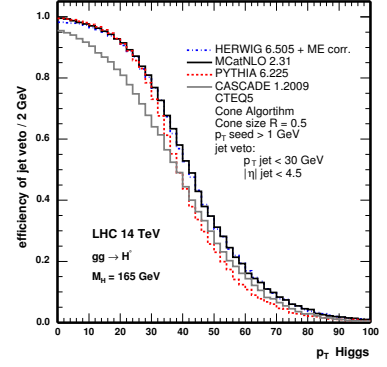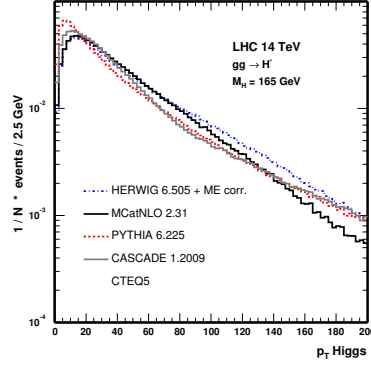
Fig. 8: Efficiency as a function of p_T for PYTHIA, HERWIG+ME Corrections, MC@NLO and CAS-CADE.

The usage of another Monte Carlo program in LHCb is important in order to estimate the uncertainty on the PYTHIA [3] predictions. In particular, the track multiplicity seen in the detector is an important factor to take into account, as it affects the performance of the trigger, the tracking and the B-tagging. But here we will concentrate on another aspect: the study of the QCD evolution itself, proving that LHCb has the potential to be a natural test bed of QCD in the forward region, complementing the studies done at present at the Tevatron and the future studies to be made with the central detectors – ATLAS and CMS – at the LHC. The predictions in the forward region as given by CASCADE are here compared with that of PYTHIA, the default Monte Carlo generator used in LHCb. This is a "natural" way to test CCFM versus DGLAP QCD evolution in the region of the phase space where differences are most likely to show.

In what follows we will compare both predictions for the event kinematics and topology, and the particle and jet production. We used CASCADE version 1.2009 "out of the box" and PYTHIA 6.227 with the LHCb tune. We used for the comparisons a sub-sample of the QCD processes of PYTHIA, as CASCADE only includes (unintegrated) gluons. PYTHIA was run with the only sub-processes $fg \rightarrow fg$, $gg \rightarrow ff$ and $gg \rightarrow gg$, and multiple interactions (MI) were also switched off, since they are as yet not implemented in CASCADE; this version is denoted *"PYTHIA gluon"* in the plots. Another configuration named *"PYTHIA gluon incl MI"* has the multiple interactions switched on, for a cross-check of the influence of such inclusion. All the plots refer to minimum bias events.

4.1 Event Kinematics

Figure 9 shows the kinematic variables Q^2 and Bjorken-x variables x_1 and x_2 (referring to both LHC proton beams of energy E_p), using the definitions given below. For PYTHIA the standard definitions from the PYPARS common block were used:

$$x_1 = \text{PARI(33)} \quad x_2 = \text{PARI(34)};$$
$$Q^2 = \text{PARI(18)},$$

whereas for CASCADE we set [5]:

$$x_{1,2} = \frac{(E + |p_z|)_{in.\ parton\ 1,2}}{2E_p};$$

---

[5]The two incoming partons in the hard interaction are obtained from the variables NIA1 and NIA2, corresponding to the positions 4 and 6 in the CASCADE event record, whereas the outgoing partons are at positions 7 and 8.
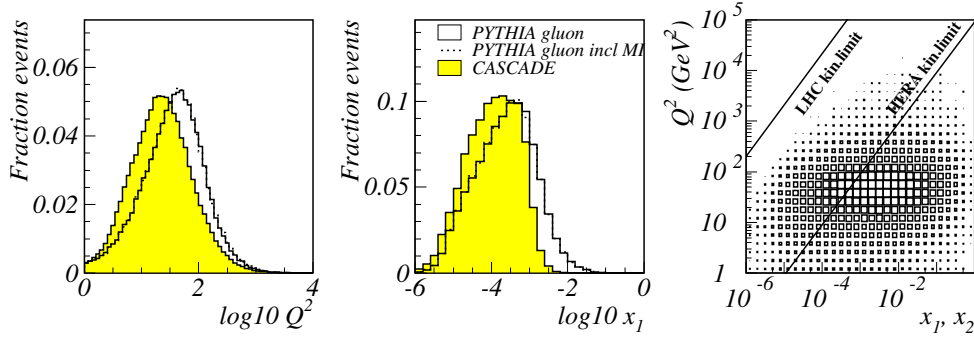
Fig. 9: Comparison between CASCADE and PYTHIA for the general event kinematics variables (refer to the text for the definitions). Note that $x_1 < x_2$ by construction.
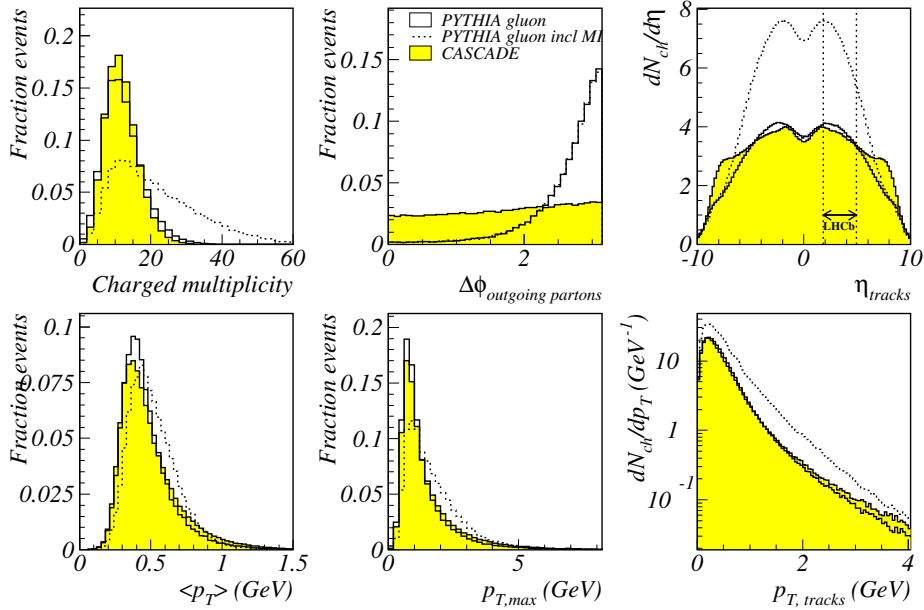

Fig. 10: Comparison between CASCADE and PYTHIA for general event variables, and between charged tracks variables in the region of the LHCb acceptance defined as $1.8 < \eta < 4.9$. No acceptance cuts are applied on the $\Delta\phi$ and η_{tracks} distributions.

$$Q^2 = p^2_{T \; out. \; parton}.$$

There is a reasonable agreement between both Monte Carlo programs, although a direct comparison seems difficult and unnatural given the definitions above. The phase space spanned by the kinematic variables $x_{1,2}$ and Q^2 is shown also in Fig. 9 for PYTHIA.

4.2 Forward Particle Production

Some general event variables are compared in Fig. 10 in the region of the LHCb acceptance, $1.8<\eta<4.9$, including the charged track multiplicity, the acoplanarity ($\Delta\phi$) of the outgoing partons, the average track transverse momentum in the event $<p_T>$ and the maximum track transverse momentum $p_{T,max}$. The predictions from both Monte Carlo programs agree well – neglecting the multiple interactions in PYTHIA – likely because the same final state parton showering is performed. The effect of including the multiple interactions is seen mainly in the event multiplicity, as expected. Interesting is the distribution of the acoplanarity of the two outgoing partons: PYTHIA predicts a strong (anti-)correlation whereas CASCADE exibits a distribution that is nearly flat.
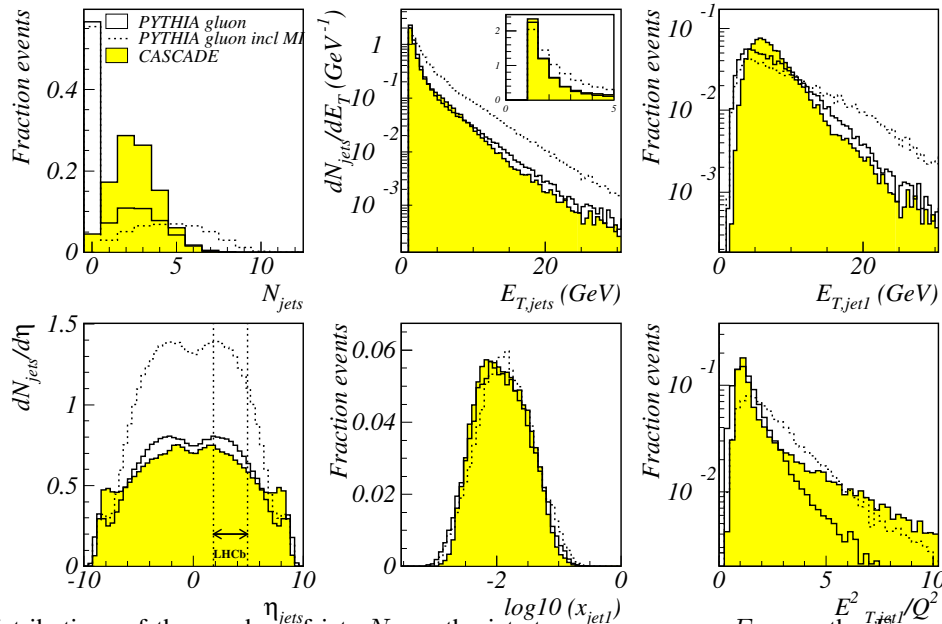
Fig. 11: Distributions of the number of jets N_{jets}, the jets transverse energy $E_{T,jets}$, the E_T and x_{jet} of the highest-E_T jet, $jet1$, all in the LHCb acceptance. Also the number of jets per unit pseudorapidity is shown. The distribution of the ratio of $E^2_{T,jet}/Q^2$ in the LHCb acceptance shows a comparison of the two scales. Jets were selected with $E_{T,jet} > 1$ GeV.

The number of charged tracks per unit rapidity, $dN/d\eta_{tracks}$, and the differential distribution of the number of charged tracks (in the LHCb acceptance) as a function of the transverse momentum $p_{T,tracks}$ are also included in Fig. 10. Note that these 2 distributions were normalized to the mean track multiplicity in the full and LHCb acceptance, respectively. The p_T distributions compare very well, leading us to conclude that the general hard dynamics of the event is predicted in a rather similar way by both programs. CASCADE however, produces more forward tracks than PYTHIA, as the η-distribution is clearly flatter than the rather steep distribution of PYTHIA. This is particularly true in the region $5 < \eta < 8$, just beyond the acceptance of the LHCb spectrometer – shown between the 2 vertical dashed lines – , but could make LHCb a candidate environment to discriminate between the two predicted forward behaviours.

4.3 Forward Jet Production

We have also looked at jet production. Jets were found in the laboratory frame with the KTCLUS algorithm on all stable hadrons, in the longitudinally invariant inclusive mode. We looked at the jet production in the LHCb acceptance with a rather loose selection of $E_{T,jets} > 1$ GeV. The number of jets found in PYTHIA or CASCADE is shown in Fig. 11. The number of events with no jets satisfying $E_{T,jet} > 1$ GeV inside $1.8 < \eta < 4.9$ is much larger for PYTHIA. In other words, CASCADE predicts a jet cross-section larger than PYTHIA, a fact already shown by the HERA experiments in low-x jet analyses. This difference leads us to believe that strong angular ordering in CASCADE favours a "clustered production" of particles and therefore the production of jets, whereas PYTHIA tends to give a more spreaded transverse energy flow. Furthermore, though the effect is small, we already saw from Fig. 10 that the highest-p_T track is somewhat softer in PYTHIA compared to CASCADE.

The rapidity distribution and the transverse energy distribution of the jets is also shown in Fig. 11; they have been normalized to the average number of jets per event in the full acceptance and LHCb acceptance, respectively. PYTHIA and CASCADE predict similar jets in the LHCb acceptance, but the inclusion of multiple interactions gives a harder spectrum.

12

Also shown are the event distributions in the LHCb acceptance of the highest-E_T jet in the event, $E_{T,jet1}$, and the energy fraction of the proton carried by the highest-E_T jet, $x_{jet1} = E_{jet1}/E_p$. The hardest jet in the event is on average harder in CASCADE compared to PYTHIA. The distributions of x_{jet} and $E_{T,jet}^2/Q^2$ are interesting in that they correspond to variables now in standard use within the HERA experiments as a means of selecting samples where forward effects are expected. Indeed both experiments have published a series of "forward QCD" analyses [25] applying cuts of the kind $E_{T,jet}^2 \sim Q^2$ and $x_{jet} \gg x_{Bjorken}$. The phase space is selected such that it suppresses jet production via DGLAP evolution and enhances production from BFKL dynamics:

- DGLAP evolution is suppressed in the small phase space for Q^2 evolution requiring $E_{T,jet}^2 \sim Q^2$;
- CCFM evolution enhanced when large phase space for x evolution requiring $x_{jet} \gg x_{Bjorken}$.

At the LHC such a selection becomes rather delicate, since there are two proton beams and the comparison of x_{jet} with $x_{Bjorken}$ gets an ambiguity between the choice of x_1 or x_2. A way out – though it lowers significantly the statistics – would be to make the selection based on $x_{jet} \gg max(x_1, x_2)$. From the distributions presented in this paper we are lead to believe that such a forward selection is indeed possible. But we leave this issue open for further investigation.

5 Summary

Various ways of treating parton showers have been compared, as implemented by the HERWIG, PYTHIA and ARIADNE Monte Carlo programs. We have studied the uncertainties that arrise from these different models to the p_T-spectrum of the jets, and the p_T-spectrum of the Higgs boson.

The theoretical systematic uncertainty on predictions for inclusive cross section at NNLO for Higgs production with bbH Yukawa coupling is under good theoretical control with an uncertainty of about 15% for a Higgs mass around 120 GeV. However, the predictions for the exclusive cross section determined by the event selection of a simplified experimental analysis indicates at present an order by magnitude larger uncertainty in e.g. $H \to \tau\tau$ events. Uncertainties due to the shower model can reach 170% and depend strongly on the production mechanism. Another factor of two arises from the choice of the QCD scale. Higher order Monte Carlo generators will therefore be mandatory to achieve better precision on the theoretical predictions.

On the other hand, the uncertainty of the jet veto efficiency in the $H \to WW \to l\nu l\nu$ decay channel by using different Monte Carlo generators in the $gg \to H$ process is estimated to be around 10%. Including higher order QCD corrections does not enhance the uncertainty significantly. Also the effect of including a realistic jet-E_T resolution is very small. The effect of including an underlying event in the simulation is smaller than 1%, and does not vary significantly for various tuning models.

Furthermore we have studied the predictions at the LHC using the CCFM formalism as implemented in the full hadron level Monte Carlo generator. We conclude that CASCADE produces more and harder jets compared to the other Monte Carlo programs, leading to a bigger uncertainty of the jet veto efficiency in the small p_T^{Higgs} range. In the forward region larger differences are expected between the DGLAP and CCFM approach, but in the moderate forward rapidity range $2 < \eta < 5$, as covered by the LHCb detector, a fairly good agreement between CASCADE and PYTHIA is observed for most of the distributions looked at, and despite their different philosophies. However, this result has to be treated with care, as the program is only recently developed for proton physics at such high energies as produced in the future LHC. It also comes out of this simple study that CASCADE is indeed a potential Monte Carlo tool to use for QCD studies at the LHC in the forward region. In the future one should further investigate regions of phase space where large differences in behaviour are expected at the LHC from DGLAP and BFKL dynamics. LHCb seems a natural experimental environment in which to study such differences.

Finally, we would like to encourage the community by stating that it is very interesting and instruc-

tive to study the predictions at the LHC by using tools developed and tuned at HERA, such as the CCFM Monte Carlo CASCADE, and by using parton shower models such as ARIADNE, that have proven their validity at HERA.

References

[1] S. Höche *et al.*, *Matching parton showers and matrix elements*. These proceedings.

[2] G. Corcella *et al.*, JHEP **0101**, 010 (2001).

[3] T. Sjöstrand *et al.*, Comput. Phys. Commun. **135**, 238 (2001).

[4] L. Lönnblad, Comput. Phys. Commun. **71**, 15 (1992).

[5] ZEUZ Collaboration, S. Chekanov *et al.*, Eur. Phys. J. **C27**, 531 (2003).

[6] S. Frixione and B. Webber, JHEP **0206**, 029 (2002).

[7] V. Gribow and L. Lipatov, Sov. J. Nucl. Phys. **15**, 438 and 675 (1971);
G. Altarelli and G. Parisi, Nucl. Phys. **B126**, 298 (1977);
Y. L. Dokshitzer, Sov. Phys. JETP **46**, 641 (1977).

[8] M. Ciafaloni, Nucl. Phys. **B296**, 49 (1988);
S. Catani, F. Fiorani, and G. Marchesini, Nucl. Phys. **B336**, 18 (1990).

[9] H. Jung, Comput. Phys. Commun. **143**, 100 (2002).

[10] J. Collins *et al.*, *Unintegrated parton density functions*. These proceedings.

[11] R. Harlander and W. Kilgore, Phys. Rev. **D68**, 013001 (2003).

[12] J. Campbell, R. K. Ellis, F. Maltoni, and S. Willenbrock, Phys. Rev. **D67**, 095002 (2003). `hep-ph/0204093`.

[13] ATLAS Collaboration, *Detector performance and physics potential TDR*, 1999. CERN-LHCC-99-15, vol.II, ch.19.

[14] E. Richter-Was, T. Szymocha, and Z. Was, Phys. Lett. **B589**, 125 (2004). `hep-ph/0402159`.

[15] E. Richter-Was, *AcerDET: a particle level fast simulation and reconstruction package for phenomenological studies on high p_t physics at LHC*. Preprint hep-ph/0207355, 2002.

[16] B. Kersevan and E. Richter-Was, *The Monte Carlo event generator AcerMC 2.0 with interfaces to PYTHIA 6.2 and HERWIG 6.5*. Preprint hep-ph/0405247, 2004.

[17] *LHAPDF online manual*, available on `http://durpdg.dur.ac.uk/lhapdf`.

[18] M. Dittmar and H. Dreiner, Phys. Rev. **D55**, 167 (1997).

[19] G. Davatz, G. Dissertori, M. Dittmar, M. Grazzini, and F. Pauss, JHEP **05**, 009 (2004).

[20] CMS Collaboration, *CMS TDR 6.2*, 2002. CERN-LHCC-2002-26, ch.15, p.317.

[21] G. Corcella and S. Moretti, Phys. Lett. **B590**, 249 (2004).

[22] S. Catani, D. de Florian, and M. Grazzini, JHEP **0105**, 025 (2001);
R. V. Harlander and W. B. Kilgore, Phys. Rev. **D64**, 013015 (2001);
R. V. Harlander and W. B. Kilgore, Phys. Rev. Lett. **88**, 201801 (2002);
C. Anastasiou and K. Melnikov, Nucl. Phys. **B646**, 220 (2002);
C. Anastasiou and K. Melnikov, Phys. Rev. Lett. **93**, 262002 (2004);
J. S. V. Ravindran and W. L. van Neerven, Nucl. Phys. **B665**, 325 (2003).

[23] I. D. A. Moraes, C. Buttar and P. Hodgson, available on `http://amoraes.home.cern.ch/amoraes/`. ATLAS internal notes.

[24] R. Field, available on `http://www.phys.ufl.edu/rfield/cdf/`. CDF Note 6403.

[25] ZEUS Collaboration, S. Chekanov *et al.* (2005). `hep-ex/0502029`;
H1 Collaboration, C. Adloff *et al.*, Nucl. Phys. **B38**, 3 (1999).

[26] LHCb Collaboration, *LHCb reoptimized detector design and performance TDR*, 2003. CERN-LHCC-2003-030.